JOC The Journal of Organic Chemistry

Article

pubs.acs.org/joc

Regiospecific Photocyclization of Mono- and Bis-Styryl-Substituted N-Heterocycles: A Synthesis of DNA-Binding Benzo[c]quinolizinium Derivatives

Tseimur M. Aliyeu,[†,‡] Daria V. Berdnikova,[*,†,‡] Olga A. Fedorova,[†] Elena N. Gulakova,[†] Christopher Stremmel,[‡] and Heiko Ihmels[‡]

[†]A. N. Nesmeyanov Institute of Organoelement Compounds, Russian Academy of Sciences, 28 Vavilova str., 119991 Moscow, Russia

[‡]Department Chemie-Biologie, Organische Chemie II, Universität Siegen, Adolf-Reichwein-Str. 2, 57068 Siegen, Germany

Supporting Information

ABSTRACT: Regiospecific C−N photocyclization of mono- and bis-styryl-substituted N-heterocycles was investigated. We demonstrated that the C−N regiospecificity of the photoinduced electrocyclization is a general feature of *ortho*-styryl-substituted N-heterocycles comprising one and two nitrogen atoms. This phototransformation provides a straightforward synthesis of the pharmaceutically important benzo[*c*]-quinolizinium cation and its aza-analogues. Noticeably, bis-styryl derivatives undergo only one-fold cyclization with the second styryl fragment remaining uninvolved in the cyclization process. Photocyclization products of monostyryl derivatives intercalate into calf thymus DNA (ct DNA), whereas photocyclization products of bis-styryl derivatives possess a mixed binding mechanism with ct DNA. The results can be used for development of novel DNA-targeting chemotherapeutics based on benzo[*c*]quinolizinium derivatives.

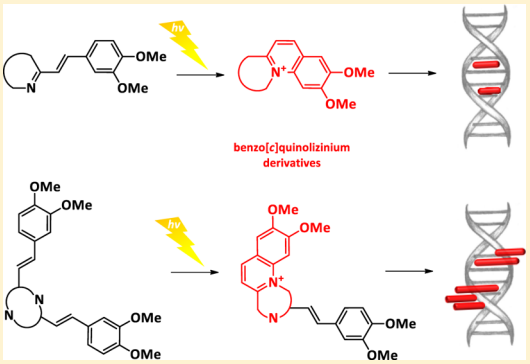

INTRODUCTION

Benzo[*c*]quinolizinium derivatives represent a pharmacologically important class of heteroaromatic compounds that is applied in clinical practice.[1] In particular, benzo[*c*]-quinolizinium (often referred to as MPBs) drugs are used as pharmacological chaperons[2] that promote folding and channel activation of the mutant CFTR protein (cystic fibrosis transmembrane conductance regulator) in the treatment of mucoviscidosis.[3] As efficient CFTR activators, benzo[*c*]-quinolizinium compounds produce a relaxing effect on tracheal[4] and aortic[5] smooth muscle cells, thus inducing bronchodilation and vasorelaxation. Because of these favorable properties, a range of benzo[*c*]quinolizinium derivatives has been patented for the use in the treatment of diseases that are linked to smooth muscle cell constriction.[6] In addition, DNA-binding properties of benzo[*c*]quinolizinium ions[7] as well as their inhibitory activity for protein kinase CKII[8] make them promising lead structures for the development of novel anticancer chemotherapeutic agents.

The first synthesis of the benzo[*c*]quinolizinium system was performed in 1958 by Glover and Jones from cyanoquinolines in three steps.[9] Later, Fozard and Bradsher obtained a series of benzo[*c*]quinolizinium derivatives by thermal cyclization of *cis*-2′-chloro-2-stilbazoles.[10] Arai et al. developed a photochemical approach toward cyclization of chloro-substituted stilbazoles.[11] Modified Ca^{2+}-assisted thermal cyclization of halogenated phenylazopyridine and related Schiff bases was applied for the synthesis of 5-aza, 6-aza, and 5,6-diaza analogues of benzo[*c*]quinolizinium.[12] Another approach to synthesize a family of 5,6-diaza-benzo[*c*]quinolizinium compounds is based on proton-catalyzed cyclization of 2-(arylazo)pyridines.[13] A series of substituted benzo[*c*]quinolizinium derivatives was prepared by condensation of 2-picolyllithium and *ortho*-halogenobenzonitrile with subsequent thermally induced cyclization.[3a] Some benzo[*c*]quinolizinium derivatives can be obtained by a ring-closing metathesis (RCM) reaction.[14] More recently, a range of novel benzo[*c*]quinolizinium salts was synthesized by interaction of α-oxoketene *S*,*S*-acetals with 2-methylquinolyllithium or 2,4-dimethyl-6-methoxyquinolyl-lithium followed by BF_3-assisted cycloaromatization.[15] However, all the reported methods possess at least one of the following significant drawbacks, namely performance of the reactions at high temperature, requirement of a catalyst (acid, Ca^{2+}), need of halogenation of the substrates at certain positions, or multistep reaction sequences.

We are developing regiospecific C−N photocyclization of hetarylphenylethenes resulting in the formation of charged polycyclic heteroaromatics.[16−21] In this reaction, a new C−N bond is formed through the photoinduced electrocyclic ring closure followed by *in situ* oxidation of the resulting dihydrohetarene intermediate by air oxygen. The process

Received: July 14, 2016
Published: September 1, 2016

DOI: 10.1021/acs.joc.6b01695
J. Org. Chem. 2016, 81, 9075−9085

Scheme 1. Photocyclization of Monostyryl Derivatives 1a−1e and Chemical Structures of Annelated Quinolizinium Derivatives 6 and 7

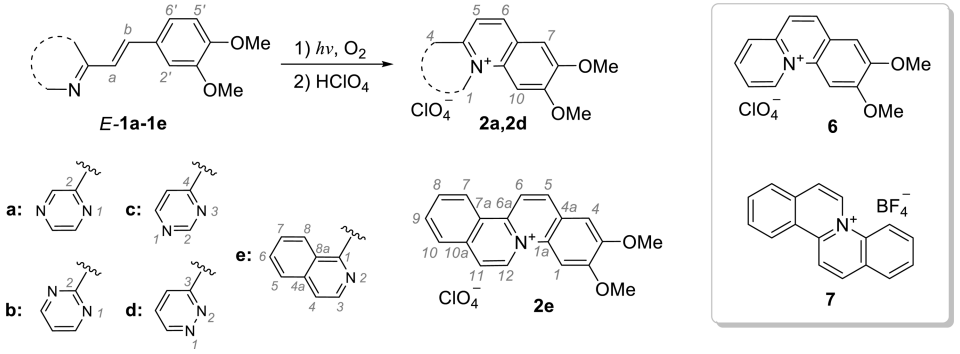

Scheme 2. Photoreactions of Bis-Styryl Derivatives 3a and 3b

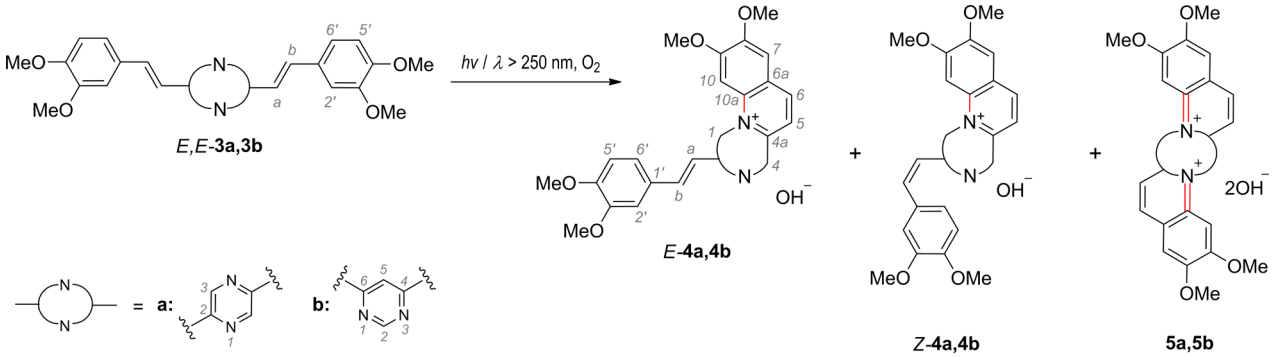

takes place under mild conditions at room temperature, does not require the use of catalysts, and allows to obtain fused polycyclic cations with good yields. Recently, we have shown that the C−N photocyclization of 2-styrylpyridine[21] and 2-styrylquinolines[19] leads to the efficient and selective formation of benzo[*c*]quinolizinium derivatives. Notably, we performed the photogeneration of the DNA-binding 8,9-dimethoxybenzo-[*c*]quinolizinium derivative **6** as a key process in a five-component supramolecular cascade. In this system, the light-controlled transport of the *in situ*-modified ligand **6** between cyclodextrin, duplex DNA, and cucurbituril was accomplished; thus demonstrating biocompatibility of this reaction (Scheme 1).[21]

Analysis of our previous data as well as the recent report of Budyka et al. on the photocyclization of styrylbenzoquinolines[22] led us to the assumption that the regioselective C−N bond formation in the photochemical cyclization may be a general chemical reactivity of *ortho*-styryl-substituted N-hetarenes containing donor substituents in the styryl residue. If that is the case, this simple reaction would open a straightforward synthesis of a wide range of biologically active benzo[*c*]quinolizinium derivatives.

As a proof of our hypothesis, we describe herein the regiospecific C−N photocyclization of mono- and bis-dimethoxystyryl-substituted N-heterocycles to the corresponding benzo[*c*]quinolizinium derivatives (Schemes 1 and 2). The substrates **1a−1e** and **3a**, **3b** were prepared by Knoevenagel condensation of the corresponding methyl-substituted heterocycles with veratraldehyde in the presence of KOBu^t in DMF (Scheme S1, Supporting Information). The methoxy groups were introduced because our previous studies showed that these substituents provide highly efficient photocyclization.[19]

Since annelated quinolizinium ions represent important key structures for the design of DNA-targeting ligands,[23] we particularly focused our attention on the interactions of the photocyclization products with DNA.

RESULTS AND DISCUSSION

Photocyclization of Monostyrylazines 1a−1e. The photocyclization reactions of monostyryl derivatives **1a−1e** (Scheme 1) were carried out in air-saturated solutions in acetonitrile or water upon irradiation with direct or filtered light of a high-pressure Hg vapor lamp; and the course of the photoreaction was monitored photometrically. Direct irradiation of dimethoxystyryl derivatives of pyrazine **1a**, pyridazine **1d**, and isoquinoline **1e** in acetonitrile led to the appearance of new red-shifted absorption bands at 350−450 nm (Figures S1, S4, and S5, Supporting Information). These bands were assigned to the photocyclization products **2a**, **2d**, and **2e** by analogy to our previous reports.[16−21] The regioselective formation of a new C−N bond in all cases was unambiguously proven by the ^{1}H NMR spectroscopic data based on the characteristic downfield shifts of the aromatic proton signals that clearly indicate the formation of the quinolizinium structure (Figures S11−S34, Supporting Information). No products of C−C cyclization were detected. The remarkable regiospecificity of this photoreaction is caused by the significantly lower enthalpy of formation of the C−N cyclization product in comparison to that of C−C cyclization product formation, as was described previously for 2-styrylquinoline derivatives.[19] Moreover, no positional isomerism of the methoxy substituents was detected for photocyclization products **2a**, **2d**, **2e**, *E*-**4a**, and *E*-**4b**. This means that formation of a new bond takes place only between N and C6′

DOI: 10.1021/acs.joc.6b01695
J. Org. Chem. 2016, 81, 9075−9085

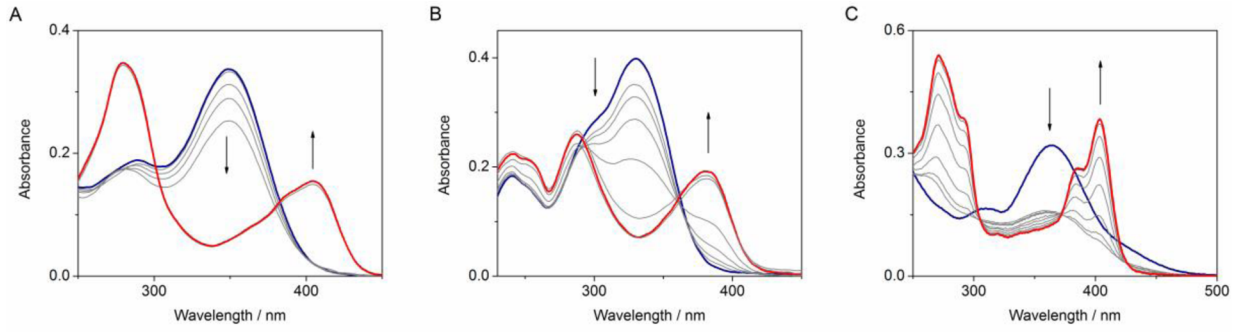

Figure 1. Spectral changes during the photolysis of **1a**, **1d**, and **1e** (c = 20 μM, water, high-pressure Hg lamp, 20 °C): (A) **1a**, λ > 290 nm, 95 min; (B) **1d**, no filter, 16 min; (C) **1e**, no filter, 15 min.

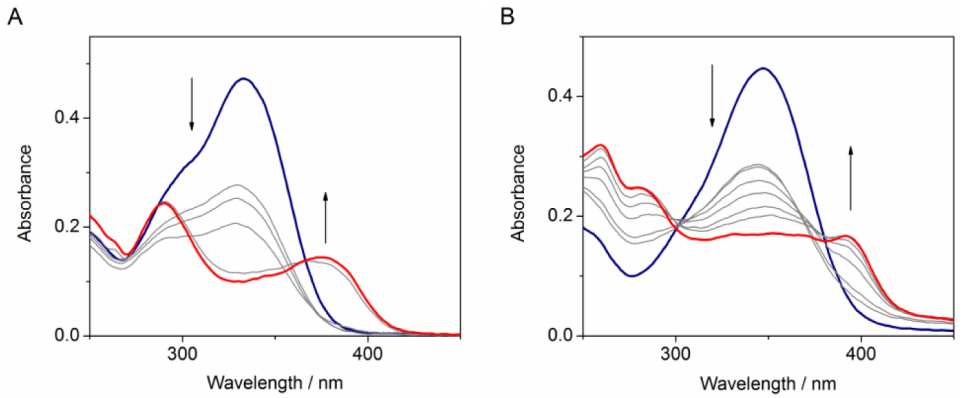

Figure 2. Spectral changes during the photolysis of **1b** and **1c** in water (c = 20 μM, high-pressure Hg lamp, 20 °C): (A) **1b**, λ > 290 nm, 35 min; (B) **1c**, no filter, 15 min.

atoms of the styrylheterocycles (Schemes 1 and 2). Considering that the electrocyclization occurs from the *Z*-form of **1** and **3**, the stability of different conformations of the corresponding *Z*-isomers influences the structure of the resulting polycyclic product. Thus, in the conformation of the *Z*-isomer that results in the N−C2′ cyclization, one of the methoxy groups in the phenyl ring is directed toward the heterocyclic fragment. This arrangement, however, leads to increased steric repulsion and destabilizes the corresponding conformation. On the other hand, in the conformation of the *Z*-isomer that leads to N−C6′ cyclization, the steric interactions are minimized so that the formation of a new bond between N and C6′ atoms is energetically favored. The monostyryl derivatives **1b**−**d**, the bis-styryl derivative **3b**, and all photocyclization products **2a**, **2d**, **2e**, *E*-**4a**, and *E*-**4b** are novel compounds and were fully characterized by NMR spectroscopy and HRMS.

Photolysis of **1a**, **1d**, and **1e** in water under similar conditions resulted in formation of more intense absorption bands of products **2a**, **2d**, and **2e** (Figure 1) as compared to the photoreaction in acetonitrile. This fact points out higher efficiencies of the photocyclization in aqueous solution. Optimization of the conditions revealed that in case of compound **1a**, the use of a cutoff filter (λ > 290 nm) leads to an enhanced yield of photoproduct **2a**. However, the removal of the short-wavelength light increased the conversion time of **1a** by ca. 2.7. Heteroaromatic compounds **2a**, **2d**, and **2e** were successfully isolated as perchlorate salts in moderate yields (**2a**: 39%; **2d**: 57%; **2e**: 50%) by recrystallization from MeOH with addition of equimolar amount of $HClO_4$.

In contrast, direct irradiation of styrylpyrimidine derivatives **1b** and **1c** in acetonitrile led to broad, almost shapeless spectra, indicating extended photodecomposition that was confirmed by the NMR spectroscopic analysis of the photolysate (Figures S2, S3, S9, S10, Supporting Information). To improve the yield of the desired photoproducts, we irradiated **1b** and **1c** in aqueous solution. The absorption spectra obtained after photolysis in water revealed pronounced red-shifted bands in the characteristic absorption range of the benzo[*c*]quinolizinium (Figure 2). Nevertheless, the isolation of the products **2b** and **2c** from the photolysate was not successful. For this reason, the obtained solutions were analyzed by HPLC (Figures S6 and S7, Supporting Information). Unfortunately, the complexity of the product mixtures, comprising at least four components with close retention times, did not allow unambiguous determination of their composition. It was obvious, however, that even if the desired products **2b** and **2c** were formed, their content in the complex mixtures was very low, and any attempts of their isolation had no preparative meaning. The most probable reason for this observation is the photochemical instability of compounds **2b** and **2c** that—unlike **2a**, **2d** and **2e**—undergo side reactions or secondary photoreactions in the course of the photolysis. In particular, it is known that pyrimidine derivatives possess low photostability and may undergo a [2 + 2] photocycloaddition reaction resulting in the formation of the intermolecular dimers.[24] To check this assumption, a control experiment was performed with the photolytic mixture obtained after irradiation of styrylpyrazine derivative **1a** in water (λ > 290 nm) (Figure 1A). In this case only two fractions were separated by HPLC with significantly different retention

DOI: 10.1021/acs.joc.6b01695
J. Org. Chem. 2016, 81, 9075−9085

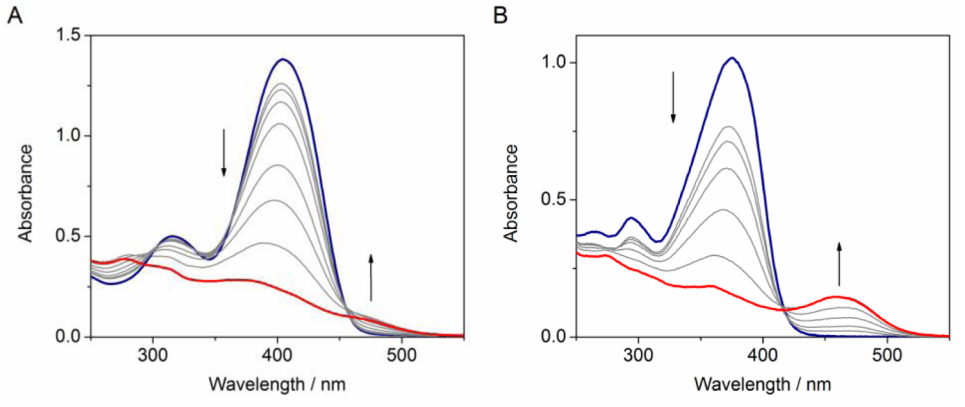

Figure 3. Spectral changes during the photolysis of the bis-styryl derivatives in acetonitrile (c = 20 μM, unfiltered light of a high-pressure Hg vapor lamp, 20 °C): (A) **3a**, 30 min; (B) **3b**, 16 min.

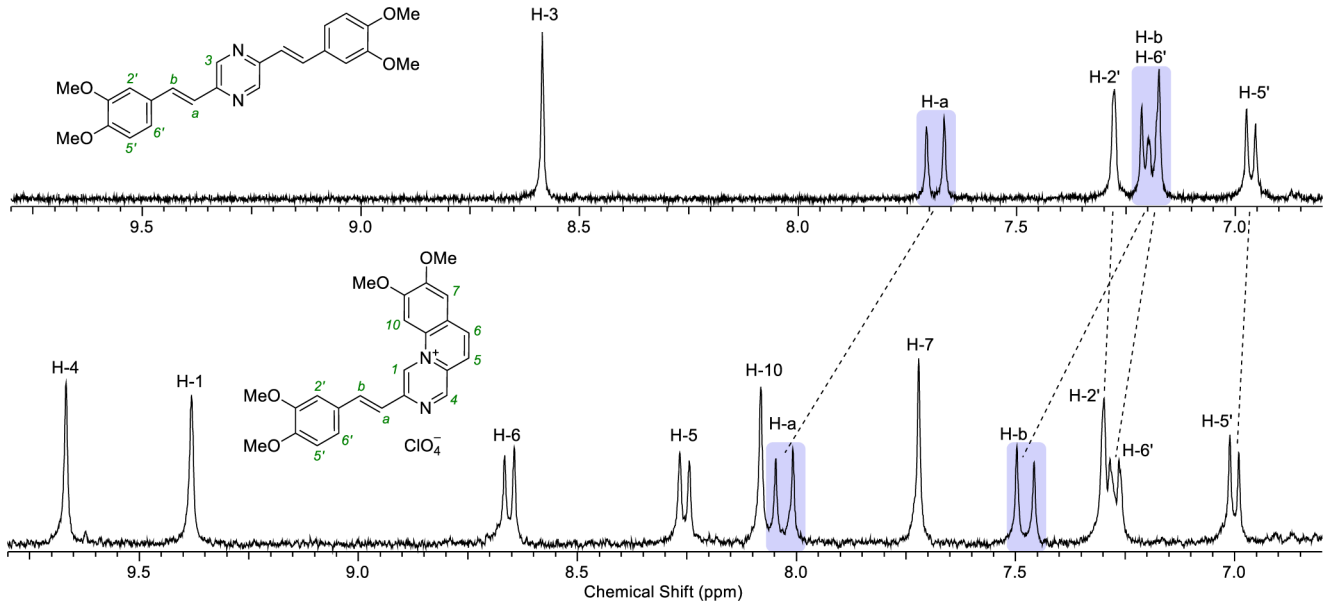

Figure 4. ^{1}H NMR spectra (400 MHz, range of the aromatic and olefin bond protons) of bis-styryl derivative *E*-**3a** (top) and its photocyclization product *E*-**4a** (bottom) in CD_3CN. The signals of the *trans*-double bonds are highlighted in blue. Dashed lines show shifting of the signals of the styryl fragment protons of photoproduct *E*-**4a** in comparison to the ones of the substrate **3a**.

times (Figure S8, Supporting Information). The absorption spectra of the obtained fractions coincide well with the absorption spectra of substrate **1a** and its photocyclization product **2a**. This observation confirmed the low stability of pyrimidine derivatives during the photolysis in comparison to other monostyrylazines from the employed series.

Photocyclization of Bis-Styrylazines 3a and 3b. Fused bis-styryl derivatives of pyrazine **3a** and pyrimidine **3b**, with both styryl moieties located in the *ortho*-positions to the nitrogen atoms of the central azine ring, are potentially capable of 2-fold C−N cyclization (Scheme 2). Two possible types of C−N electrocyclization products for **3a**, **3b** can be suggested with only one or both styryl fragments involved in the cyclization yielding corresponding mono- and dicationic heteroaromatics **4a**, **4b** and **5a**, **5b**. It should be noted that the dimethoxystyryl fragment of monocationic species **4a** and **4b** can potentially exist in *E*- or *Z*-form.

Direct irradiation of the acetonitrile solutions of bis-styrylpyrazine **3a** and bis-styrylpyrimidine **3b** under aerobic conditions resulted in the formation of the red-shifted absorption bands that indicate the extension of a conjugated aromatic system in the course of the photoreaction (Figure 3). The photolysate was purified by recrystallization from MeOH in the presence of $HClO_4$. As a result, pure *E*-isomers of monocyclization products **4a**, **4b** were isolated as perchlorate salts with low to moderate yields (*E*-**4a**: 25%; *E*-**4b**: 51%). Neither *Z*-isomers of **4a**, **4b** nor dicationic species **5a**, **5b** were detected (Figure 4). Interestingly, irradiation of **3a** and **3b** with filtered light (λ = 405 nm for **3a** or λ = 365 nm for **3b**) did not lead to the formation of polycyclic products. The poor solubility of **3a** and **3b** in water did not allow us to test the photocyclization process in aqueous medium.

The inhibition of the photoinduced *E*−*Z*-isomerization in **4a** and **4b** unambiguously points out the presence of an alternative dominating relaxation pathway in the excited state. Indeed, compounds **4a** and **4b** resemble cationic styryl dyes with a highly polar donor−acceptor structure that upon photoexcitation in polar media readily undergo nonradiative relaxation through rotation about single bonds and formation of twisted excited states.[25] In such systems, *E*−*Z*-isomerization

DOI: 10.1021/acs.joc.6b01695
J. Org. Chem. 2016, 81, 9075−9085

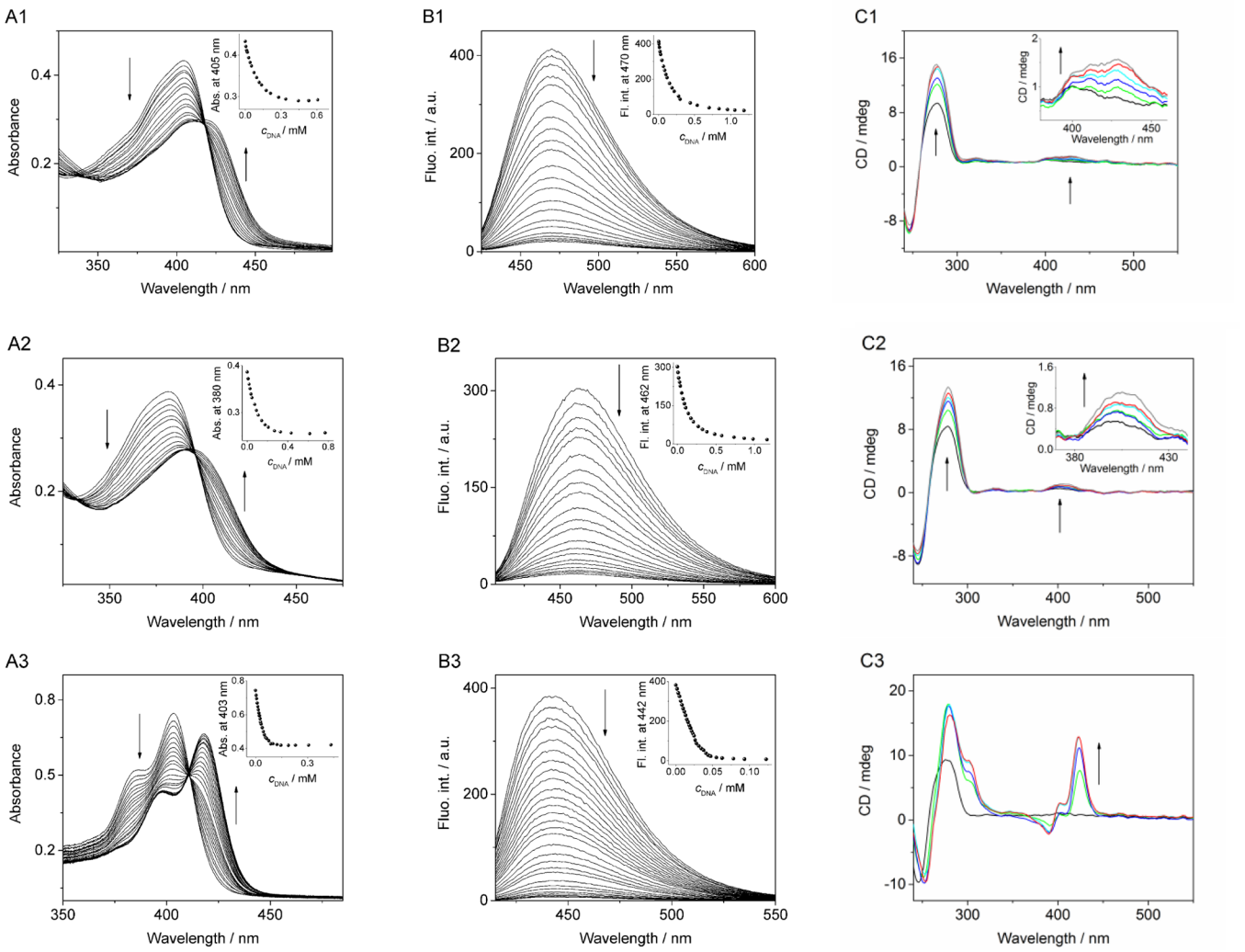

Figure 5. (A) Spectrophotometric titration of ct DNA to **2a** (A1, c_{2a} = 50 μM, c_{DNA}/c_{2a} = 0–21); **2d** (A2, c_{2d} = 50 μM, c_{DNA}/c_{2d} = 0–23); **2e** (A3, c_{2e} = 20 μM, c_{DNA}/c_{2e} = 0–24). (B) Fluorimetric titration of ct DNA to **2a** (B1, c_{2a} = 20 μM, c_{DNA}/c_{2a} = 0–59, λ_{ex} = 418 nm); **2d** (B2, c_{2d} = 20 μM, c_{DNA}/c_{2d} = 0–57, λ_{ex} = 396 nm); **2e** (B3, c_{2e} = 10 μM, c_{DNA}/c_{2e} = 0–14, λ_{ex} = 410 nm). (C) CD spectra of mixtures of ct DNA (c_{DNA} = 50 μM, in base pairs) with ligands **2a** (C1), **2d** (C2), **2e** (C3) at ligand-DNA ratio (LDR) = 0, 0.3, 0.6, 0.8, 1.0, 1.5. In all cases: BPE buffer (pH 7.0) with 2% v/v DMSO, T = 20 °C.

of the C=C double bonds is usually significantly suppressed. Therefore, we assume that the absence of *E*–*Z*-isomerization may be a consequence of the pronounced dipolar character of **4a**, **4b** that promotes relaxation through the twisted excited states. However, the detailed investigation of the photophysical behavior of **4a** and **4b** is beyond the scope of the present study.

The exclusive formation of **4a** and **4b** in the *E*-form provides an explanation why two-fold cyclization to **5a**, **5b** does not occur, because the cyclization can take place only from the *Z*-form of a styrylheterocyclic species.[19] Since the *Z*-isomers of **4a** and **4b** do not form, the cyclization process cannot proceed further and stops on the monocyclization stage. An additional reason for the impeded second cyclization may be the electrostatically unfavorable accumulation of two positive charges within one six-membered ring in **5a** and **5b**.

DNA-Binding Properties of Photocyclization Products 2a, 2d, 2e. The photoproducts **2a**, **2d**, and **2e** possess characteristic features of DNA-intercalators, namely, planar heteroaromatic structure with a permanent positive charge.[26] To assess DNA-binding properties of these compounds, their interaction with calf thymus DNA (ct DNA) was examined by spectrometric titrations. Thus, addition of ct DNA to the solutions of compounds **2a**, **2d**, and **2e** produced a strong hypochromic effect along with a pronounced red shift of the absorption of the ligand that is indicative of a strong interaction with DNA (Figure 5A, Table 1). In all cases, an isosbestic point is maintained during the titrations that indicates one almost exclusive binding mode. Fitting of the binding isotherms obtained from the photometric titrations to the neighbor-exclusion model[27] gave the binding constants for the complexes of **2a**, **2d**, and **2e** with ct DNA (Table 1). The binding constant of 3-azabenzo[*c*]quinolizinium derivative **2a** (K_b = 1.1 × 10^5 M^{-1}) is very close to the one reported for 8,9-dimethoxybenzo-[*c*]quinolizinium **6** (K_b = 1.2 × 10^5 M^{-1})[21] which can be explained by close structural resemblance of these compounds. At the same time, the DNA-binding affinity of structurally similar 1-azabenzo[*c*]quinolizinium derivative **2d** is slightly lower (K_b = 6.6 × 10^4 M^{-1}). The binding constant of 2,3-dimethoxy-isoquinolinoquinolinium derivative **2e** (K_b = 4.6 × 10^5 M^{-1}) is of the same order of magnitude as the one of the parent compound **7** (K_b = 1.9 × 10^5 M^{-1}).[28] Overall, the values of the binding constants of ligands **2a**, **2d**, and **2e** with ct DNA

DOI: 10.1021/acs.joc.6b01695
J. Org. Chem. 2016, 81, 9075–9085

Table 1. Absorption and Emission Maxima of Free and DNA-Bound Ligands 2a, 2d, 2e, *E*-4a, and *E*-4b and Binding Constants of Their Complexes with ct DNA in BPE buffer (pH 7.0) with 2% v/v DMSO (for 2a, 2d, 2e) or 5% v/v DMSO (for *E*-4a, *E*-4b)

	λ_{abs}/nm[a]		λ_{fl}/nm[b]		
	free	bound	free	bound	K_b/M^{-1}
2a	405	415	470	472	1.1×10^{5}[c]
2d	382	393	463	460	6.6×10^{4}[c]
2e	403	418	442	443	4.6×10^{5}[c]
E-**4a**	460	477	456	500	–[d]
E-**4b**	452	475	547	550	5.0×10^{5}[e]

[a]Long-wavelength absorption maxima of free and DNA-bound ligands. [b]Fluorescence maxima of free and DNA-bound ligands. [c]Binding constant with ct DNA, obtained from the photometric data. [d]Binding constant was not determined. [e]Average binding constant with ct DNA, obtained from the fluorimetric data that reflects the combination of two binding modes. T = 20 °C.

are in good agreement with the reported data for DNA-intercalators of similar structure and size. The fluorescence of **2a**, **2d**, and **2e** was efficiently quenched upon addition of ct DNA with almost no changes in the positions of the emission maxima (Figure 5B, Table 1), which usually indicates the photoinduced electron transfer (PET) reaction between the bound ligand and the DNA bases, specifically the easily oxidized guanine residues.[29] Complementary polarimetric titrations revealed that in the presence of ct DNA the achiral ligands **2a**, **2d** and **2e** display induced circular dichroism (ICD) signals that resemble the long-wavelength absorption of the ligands in the presence of DNA (Figure 5C). The tricyclic compounds **2a** and **2d** possess weak positive ICD signals, whereas the tetracyclic derivative **2e** exhibits a strong bisignated ICD signal that may indicate aggregation of **2e** in the presence of DNA or two energetically close orthogonal transition dipoles.[30] In particular, the positive ICD signals result from an alignment of the transition dipole of the ligands perpendicular to the long axis of the binding pocket, i.e., the direction of the transition dipole of the DNA bases.[30] At the same time, it may be assumed that the transition dipole moment of the long-wavelength absorption band of the ligands **2a**, **2d**, and **2e** is essentially pointing along their long molecular axes, i.e., from the methoxy sustituents to the pyridinium unit (Scheme 1). As a result, similarly as demonstarted for **7** already in detail,[28] it can be deduced from the positive ICD band that the ligands intercalate into DNA with their long molecular axes pointing almost perpendicular relative to the long axis of the intercalation pocket.

To verify the proposed intercalative binding mode of the heteroaromatic photoproducts **2** with ct DNA, flow-linear dichroism (LD) spectroscopic analysis[30] was performed exemplarily with ligand **2e** (Figure 6). The ct DNA without ligand gives a negative signal in the absorption region of the DNA bases (Figure 6A) as a result of the perpendicular alignment of the transition dipole moment of the bases relative to the LD reference axis.[30] The addition of ct DNA to **2e** led to formation of a negative LD signal in the absorption range of the ligand (Figure 6A). This negative LD signal of **2e** results from a parallel alignment of the transition dipole of the bound ligand and the ones of the DNA bases, thus indicating the intercalative binding mode of the planar aromatic system of the ligand.[30] Further information about the relative orientation of the ligand in the binding site of DNA is provided by the reduced linear dichroism, LD_r, i.e., the wavelength-dependent LD. In the case of DNA-bound **2e**, the LD_r values in the absorption regions of the DNA bases and of the ligand are negative and essentially independent of the absorption wavelength (Figure 6B), which confirms the intercalation of the ligand into the DNA helix.[30] Moreover, observation that the amplitude of the LD_r band of compound **2e** has almost the same magnitude than the one of the DNA bases indicates essentially coplanar alignment of the aromatic π system of the ligand to the DNA bases.

DNA-Binding Properties of Photocyclization Products *E*-4a,4b. Spectrophotometric titrations of the photoproducts *E*-**4a** and *E*-**4b** with ct DNA revealed nonuniform changes in the absorption intensity with no isosbestic point (Figure 7A). In the first part of the titration (ligand-DNA ratio (LDR): 110–7 for *E*-**4a**; 344–9 for *E*-**4b**), the absorption decreases with a small red shift of the absorption maxima for *E*-**4a** or a pronounced blue shift for *E*-**4b**, whereas at smaller LDR (<7 for *E*-**4a**; <9 for *E*-**4b**), the absorption band increases with a significant red shift. Such a behavior usually indicates the presence of at least two different binding modes. The complex changes observed during the photometric titrations of ct DNA to *E*-**4a** and *E*-**4b** represent a superposition of changes arising from the different binding modes that cannot be dissected. For this reason, calculation of the binding constant from the photometric data was not possible.

A special feature of the photometric titration of DNA to *E*-**4b** is the initial blue shift of the absorption maximum at high LDR, which is rarely observed, for example, on H-aggregate

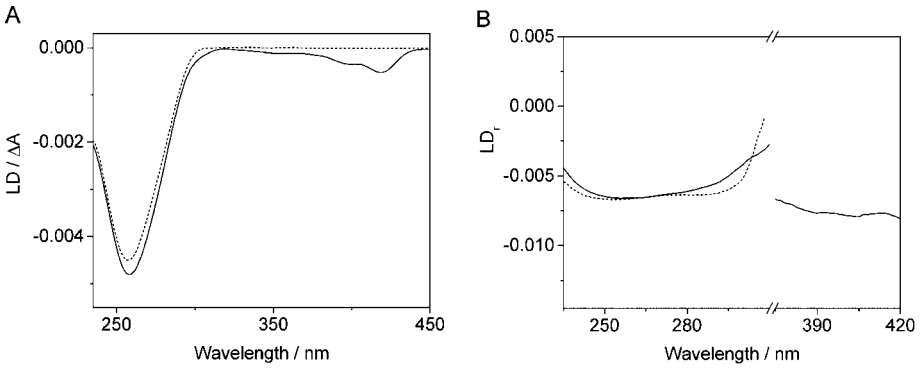

Figure 6. LD (A) and reduced LD_r (B) spectra of ligand **2e** in the presence of ct DNA (c_{DNA} = 50 μM, in base pairs) at LDR of 0 (...) and 0.04 (—) in BPE buffer (pH 7.0) with 2% v/v DMSO, T = 20 °C.

DOI: 10.1021/acs.joc.6b01695
J. Org. Chem. 2016, 81, 9075–9085

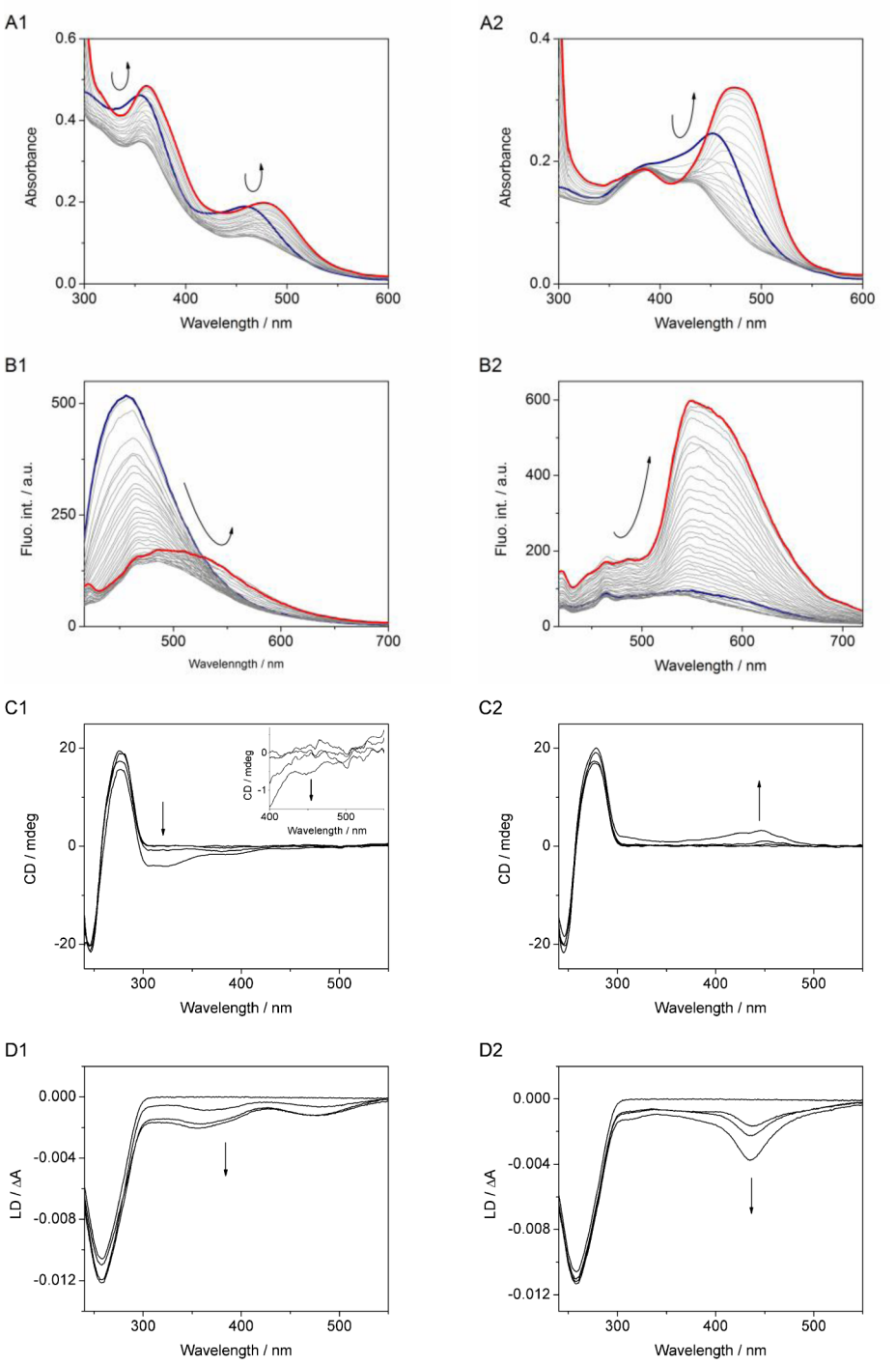

Figure 7. (A) Spectrophotometric titration of ct DNA to *E*-**4a** (A1, $c_{E\text{-}4a}$ = 50 μM, $c_{DNA}/c_{E\text{-}4a}$ = 0−13.3); *E*-**4b** (A2, $c_{E\text{-}4b}$ = 50 μM, $c_{DNA}/c_{E\text{-}4b}$ = 0−23.8). (B) Fluorimetric titration of ct DNA to *E*-**4a** (B1, $c_{E\text{-}4a}$ = 25 μM, $c_{DNA}/c_{E\text{-}4a}$ = 0−48.7, λ_{ex} = 400 nm); *E*-**4b** (B2, $c_{E\text{-}4b}$ = 25 μM, c_{DNA} $c_{E\text{-}4b}$ = 0−48.0, λ_{ex} = 400 nm). (C) CD spectra of mixtures of ct DNA (c_{DNA} = 0.1 μM, in base pairs) with ligands *E*-**4a** (C1), *E*-**4b** (C2) at LDR = 0, 0.3, 0.6, 1.2. (D) LD spectra of mixtures of ct DNA (c_{DNA} = 0.1 μM, in base pairs) with ligands *E*-**4a** (D1), *E*-**4b** (D2) at LDR = 0, 0.3, 0.6, 1.2. In all cases: BPE buffer (pH 7.0) with 5% v/v DMSO (for the photometric and fluorimetric titrations) or 7% v/v DMSO (for the CD and LD measurements), T = 20 °C. Blue lines denote the initial absorption and fluorescence spectra of *E*-**4a** and *E*-**4b**; red lines denote the corresponding spectra of DNA-bound *E*-**4a** and *E*-**4b** at saturation. Arrows indicate changes of the bands upon addition of ct DNA.

formation of cyanine dyes along the DNA backbone.[31] In the case of *E*-**4b**, however, the backbone aggregation is rather unlikely because other than the cyanine dyes, this ligand does not have the molecular shape and flexibility such that its H-aggregates fit perfectly in the DNA groove. Therefore, we assume that the blue shift is a result of a particular conformation of the DNA-bound ligand. Because of its rather rod-like structure, *E*-**4b** may have significant twist about the alkene-aryl bonds to provide a reasonable fit to the DNA binding sites. In this conformation, the styryl unit is no longer well conjugated with the quinolizinium chromophore, so that a reduced donor−acceptor interplay results a blue shift. Evidence for this assumption is provided by the observation that the absorption maximum is close to the one of the DNA-bound

DOI: 10.1021/acs.joc.6b01695
J. Org. Chem. 2016, 81, 9075−9085

benzo[*c*]quinolizinium ligands **2a** and **2d** that lack the styryl substituent.

For further investigation of the binding modes, CD- and flow-LD-spectroscopic analyses were performed (Figure 7C,D). In the case of ligand *E*-**4a**, ICD bands were detected between 300 and 400 nm upon complexation with DNA (Figure 7, C1). Most notably, only a very weak ICD bands developed in the long-wavelength absorption range of the ligand. This observation indicates that the transition dipole moments of the DNA base pairs couple efficiently with the transition dipole of the ligand that is assigned to the S_0-S_2 and/or S_0-S_3 transition (see discussion above). In contrast, the coupling with the lower energy S_0-S_1 transition appears to be very weak, presumably because of an unfavorable relative orientation of the respective transition dipoles toward each other.[30] In the flow-LD experiment, however, clear negative LD bands were recorded in the absorption region of *both* transitions of the ligand *E*-**4a** (Figure 7, D1), thus indicating the intercalation of aromatic ligands into DNA (see discussion above).[30] These observations clearly indicate that one binding mode of ligand *E*-**4a** is intercalation, as unambiguously confirmed by the negative LD bands of the ligand. In analogy to the ligands **2a** and **2d** (see above), the ligand *E*-**4a** binds to DNA with the benzo[*c*]quinolizinium fragment inserted between the DNA base pairs, whereas the dimethoxystyryl unit is pointing outside the DNA helix.

In the case of ligand *E*-**4b**, the addition of DNA led to the development of a positive ICD and a negative LD band only at ca. 450 nm (Figure 7, C2 and D2), corresponding to the blue-shifted absorption band formed at high ligand-DNA ratios, LDR > 9 (Figure 7, A2). Like in the case of *E*−*E*-**4a**, these ICD and LD bands indicate the intercalation of the benzo[*c*]-quinolizinium fragment. But remarkably, the absorption band that was observed during photometric titration at smaller LDR values (LDR < 9) is neither CD nor LD active. Such a lack of CD and LD spectroscopic response of a DNA ligand is usually the result of unspecific aggregation along the DNA backbone, however, this binding mode occurs at high LDR values and is usually negligible at low LDR. At the same time, groove binding may be considered as alternative binding mode like for related styryl dyes,[32] but groove-bound ligands usually give very strong ICD bands. Hence, along with the interpretation of the unusual blue shift during photometric titration (see above), it may be proposed that at the beginning of the titration, i.e., at high LDR, the DNA is fully loaded with intercalated molecules, each of which occupies several binding sites because a fairly large amount of the ligand points outside the binding site and hinders the approach of another ligand in its close vicinity. With decreasing LDR value, the intercalating ligands are distributed less densely over the DNA molecule, such that the ligand can also form aggregates that associate unselectively along the DNA backbone. Apparently, the binding constants of both binding modes are in the same range so that they compete at low LDR.

Despite the structural similarity of compounds *E*-**4a** and *E*-**4b**, their emission properties in the presence of ct DNA differ significantly. Thus, upon increasing the concentration of DNA, the fluorescence of *E*-**4a** was efficiently quenched with just residual increase at the end of the titration. In addition, the emission maximum exhibited a pronounced red shift in the presence of DNA ($\Delta\lambda$ = 44 nm) (Figure 7B, Table 1). By contrast, the fluorescence of *E*-**4b** lights up by a factor of 6.3 upon addition of ct DNA with a negligible red shift of the emission maximum ($\Delta\lambda$ = 3 nm) (Figure 7B, Table 1). Most likely, this diverge behavior of the two ligands arises from a different contribution of the two above-mentioned DNA binding modes in each case. By analogy to benzo[*c*]-quinolizinium intercalators **2a**, **2d**, and **2e**, whose fluorescence is completely quenched in the presence of ct DNA (Figure 5B), we assume that intercalation of the benzo[*c*]quinolizinium fragment of *E*-**4a** and *E*-**4b** between the DNA base pairs is also accompanied by fluorescence quenching due to photoinduced PET processes, as described above.[29] On the other hand, the aggregation of the cationic styryl derivatives *E*-**4b** along the DNA backbone prevents the nonradiative rotational relaxation and subsequently leads to the enhancement of the fluorescence intensity, thus representing a special case of aggregation-induced enhancement of emission.[33] Analysis of the fluorimetric data allowed to determine an average binding constant with ct DNA for *E*-**4b** (Table 1), reflecting the combination of two binding modes.

CONCLUSION

To sum up, we have demonstrated that *ortho*-styryl-substituted N-heterocycles comprising one and two nitrogen atoms generally undergo the regioselective C−N bond formation during photocyclization, resulting in formation of the family of (aza)benzo[*c*]quinolizinium derivatives. The photocyclization of monostyryl derivatives **1a**, **1d**, and **1e** occurs more efficiently in aqueous solution than in organic solvents (acetonitrile), making the process environment friendly. Bis-styryl derivatives **3a** and **3b**, although designed for the two-fold cyclization, cyclize only one styryl fragment, whereas the second styryl residue remains photochemically inert. DNA-binding studies with ct DNA revealed that all obtained photoproducts have a high affinity toward nucleic acids. Interestingly, the photoproducts **2a**, **2d**, and **2e** of monostyrylheterocycles are typical DNA-intercalators, while the photoproducts *E*-**4a** and *E*-**4b** of bis-styrylheterocycles demonstrate a mixed binding mode comprising intercalation and aggregation along the DNA backbone. Overall, the studied phototransformation is the most simple synthetic approach, so far, to the benzo[*c*]-quinolizinium scaffold that may be applied in the development of new DNA-targeting chemotherapeutics.

EXPERIMENTAL SECTION

All reagents and solvents were obtained from commercial sources and used as received. ^{1}H NMR spectra were recorded at 400 or 600 MHz, and ^{13}C NMR spectra were recorded at 101 or 151 MHz at ambient temperature using 5 mm tubes. Chemical shifts were determined with accuracy of 0.01 and 0.1 ppm for ^{1}H and ^{13}C spectra, respectively, and are given relative to the residual signal of the solvent that was used as internal reference. Spin−spin coupling constants for the proton spectra were determined with accuracy of 0.1 Hz. The ^{1}H NMR signal assignments were performed using COSY and NOESY 2D NMR techniques. The ^{13}C NMR signal assignments were performed by means of HSQC and HMBC 2D NMR techniques. Electrospray ionization (ESI) mass spectra were detected in the mode of full mass scanning of positive ions on a tandem dynamic mass spectrometer equipped with a mass analyzer with an octapole ionic trap. High-resolution mass spectra were recorded on a time-of-flight instrument in a positive-ion mode using ESI method. TLC was performed on silica gel on Al foils, eluent: EtOAc. Preparation and handling of the solutions were carried out under red light. Photochemical reactions were carried out with a high-pressure Hg vapor lamp (120 W) and an immersed Hg photoreactor (125 W). Electronic absorption spectra were measured on a fiber-optic spectrometer connected to a computer at 20 ± 1 °C. Fluorescence spectra were measured on a

DOI: 10.1021/acs.joc.6b01695
J. Org. Chem. 2016, 81, 9075−9085

spectrofluorimeter equipped with double-grating monochromators and a Xe flash lamp at 20 ± 1 °C. Circular dichroism (CD) and linear dichroism (LD) spectra were recorded on a CD spectrometer equipped with a high shear couette cell accessory (for LD measurements). The LD samples were oriented in a rotating Couette with a shear gradient of 1200 s^{-1}. The reduced linear dichroism, LD_r, was calculated according to eq 1.

$$LD_r = LD/A_{iso} \quad (1)$$

where A_{iso} is the absorbance of an isotropic sample that is determined under the same conditions as the LD.

General Procedure for the Synthesis of Monostyryl Derivatives (1a−1e) and Bis-Styryl Derivatives (3a, 3b). A mixture of 3,4-dimethoxybenzaldehyde (for monostyryl derivatives: 300 mg, 1.80 mmol; for bis-styryl derivatives: 600 mg, 3.60 mmol), the corresponding methyl-substituted heterocycle [for **1a**: 2-methylpyrazine (0.16 mL, 1.80 mmol); for **1b**: 2-methylpyrimidine (0.17 mL, 1.80 mmol); for **1c**: 4-methylpyrimidine (0.16 mL, 1.80 mmol); for **1d**: 3-methylpyridazine (0.16 mL, 1.80 mmol); for **1e**: 1-methylisoquinoline (0.24 mL, 1.80 mmol); for **3a**: 2,5-dimethylpyrazine (197 μL, 1.80 mmol); for **3b**: 4,6-dimethylpyrimidine (199 μL, 1.80 mmol)] and potassium *tert*-butoxide (for monostyryl derivatives: 202 mg, 1.80 mmol; for bis-styryl derivatives: 404 mg, 3.60 mmol) in abs. DMF (for monostyryl derivatives: 4 mL; for bis-styryl derivatives: 2.5 mL) was stirred at room temperature for 2−4 h (monostyryl derivatives) or 24 h (bis-styryl derivatives). The reaction mixture was diluted with water (2 mL) and concentrated in vacuo. The obtained solid was dissolved in water (30 mL) and extracted with dichloromethane (5 × 20 mL). The organic layers were combined, and the solvent was removed.

*(E)-2-(3,4-Dimethoxystyryl)pyrazine (**1a**).* Recrystallized from MeOH; yellow solid, yield 51% (0.91 mmol, 220 mg), mp 103−105 °C (lit. mp 107−108 °C).[34] ^{1}H NMR (DMSO-d_6, 400 MHz) δ: 3.79 (s, 3H, OCH_3), 3.84 (s, 3H, OCH_3), 6.99 (d, 1H, H-5′, J = 8.3 Hz), 7.20 (br. d, 1H, H-6′, J = 8.3), 7.28 (d, 1H, H-a, J_{trans} = 16.1 Hz), 7.34 (br. s, 1H, H-2′), 7.72 (d, 1H, H-b, J_{trans} = 16.1 Hz), 8.45 (d, 1H, H-6, J = 2.4 Hz), 8.59 (br. s, 1H, H-5), 8.75 (br. s, 1H, H-3). ^{13}C NMR (DMSO-d_6, 100 MHz) δ: 55.5 (2C, O$\underline{C}H_3$), 109.6, 111.7, 121.4, 122.2, 128.8, 134.4, 142.6, 143.5, 144.4, 149.0, 149.8, 151.1. Anal. calcd for $C_{14}H_{14}N_2O_2$: C, 69.41; H, 5.82; N, 11.56; found: C, 69.20; H, 5.81; N, 11.49. ESI-MS **1a** in MeCN, m/z: calcd 242.27; found 243.10 [**1a** + H]$^+$.

*(E)-2-(3,4-Dimethoxystyryl)pyrimidine (**1b**).* Further purification was not required; white solid, yield 53% (0.95 mmol, 230 mg), mp 110−112 °C. ^{1}H NMR (CD_3CN, 600 MHz) δ: 3.83 (s, 3H, OCH_3), 3.87 (s, 3H, OCH_3), 6.96 (d, 1H, H-5′, J = 8.3 Hz), 7.15 (d, 1H, H-a, J_{trans} = 15.9 Hz), 7.16 (t, 1H, H-5, J = 4.8 Hz, 9.6 Hz), 7.22 (d, 1H, H-6′, J = 8.6 Hz), 7.30 (s, 1H, H-2′), 7.91 (d, 1H, H-b, J_{trans} = 15.9 Hz), 8.70 (d, 2H, H-4, H-6, J = 4.8 Hz). ^{13}C NMR (CD_3CN, 151 MHz) δ: 56.6 (*m*-O$\underline{C}H_3$), 56. Seven (*p*-O$\underline{C}H_3$), 111.1 (C-2′), 112.8 (C-5′), 119.8 (C-5), 122.9 (C-6′), 126.8 (C-a), 130.2 (C-1′), 138.6 (C-b), 150.7 (C-3′), 151.7 (C-4′), 158.4 (2C, C-4, C-6), 166.1 (C-2). Anal. calcd for $C_{14}H_{14}N_2O_2$: C, 69.41; H, 5.82; N, 11.56; found: C, 69.48; H, 5.89; N, 11.61. ESI-MS **1b** in MeCN, m/z: calcd 242.27; found 243.60 [**1b** + H]$^+$. HRMS (ESI-TOF) m/z: [**1b** − H]$^+$ calcd for $C_{14}H_{13}N_2O_2$ 241.0972; found 241.0973.

*(E)-4-(3,4-Dimethoxystyryl)pyrimidine (**1c**).* Recrystallized from MeOH; yellow solid, yield 52% (0.94 mmol, 227 mg), mp 108−110 °C. ^{1}H NMR (CD_3CN, 600 MHz) δ: 3.86 (s, 3H, OCH_3), 3.90 (s, 3H, OCH_3), 6.99 (d, 1H, H-5′, J = 8.4), 7.11 (d, 1H, H-a, J_{trans} = 16.0 Hz), 7.24 (d, 1H, H-6′, J = 8.4 Hz), 7.31 (br. s, 1H, H-2′), 7.42 (d, 1H, H-3, J = 5.3 Hz), 7.88 (d, 1H, H-b, J_{trans} = 16.0 Hz), 8.66 (d, 1H, H-6, J = 5.1 Hz), 9.08 (s, 1H, H-4). ^{13}C NMR (CD_3CN, 151 MHz) δ: 56.4 (2C, O$\underline{C}H_3$), 110.9 (C-2′), 112.6 (C-5′), 119.6 (C-5), 122.9 (C-6′), 124.8 (C-a), 129.7 (C-1′), 137.8 (C-b), 150.5 (C-3′), 151.7 (C-4′), 158.5 (C-6), 159.7 (C-2), 163.5 (C-4). Anal. calcd for $C_{14}H_{14}N_2O_2$: C, 69.41; H, 5.82; N, 11.56; found: C, 69.50; H, 5.84; N, 11.56. ESI-MS **1c** in MeCN, m/z: calcd 242.27; found 243.50 [**1c** + H]$^+$. HRMS (ESI-TOF) m/z: [**1c** − H]$^+$ calcd for $C_{14}H_{13}N_2O_2$ 241.0972; found 241.0978.

*(E)-3-(3,4-Dimethoxystyryl)pyridazine (**1d**).* The residue was purified by column chromatography (SiO_2; ethyl acetate; R_f = 0.80); pale yellow solid, yield 48% (0.86 mmol, 208 mg), mp 83−85 °C. ^{1}H NMR (DMSO-d_6, 600 MHz) δ: 3.80 (s, 3H, OCH_3), 3.85 (s, 3H, OCH_3), 7.01 (d, 1H, H-5′, J = 8.4 Hz), 7.22 (dd, 1H, H-6′, J = 8.4 Hz; 2.0 Hz), 7.35 (d, 1H, H-b, J_{trans} = 16.1 Hz), 7.36 (d, 1H, H-2′, J = 2.0 Hz), 7.65 (dd, 1H, H-5, J = 8.4 Hz; 4.8 Hz), 7.73 (d, 1H, H-a, J_{trans} = 16.5 Hz), 7.90 (dd, 1H, H-4, J = 8.8 Hz; 1.6 Hz), 9.06 (dd, 1H, H-6, J = 4.8 Hz; 1.2 Hz). ^{13}C NMR (DMSO-d_6, 151 MHz) δ: 55.50 (3′-O$\underline{C}H_3$), 55.52 (4′-O$\underline{C}H_3$), 109.8 (C-2′), 111.8 (C-5′), 121.2 (C-6′), 123.1 (C-a), 123.9 (C-4), 126.8 (C-5), 128.8 (C-1′), 134.5 (C-b), 149.0 (C-3′), 149.6 (C-6), 149.8 (C-4′), 158.1 (C-3). Anal. calcd for $C_{14}H_{14}N_2O_2$: C, 69.41; H, 5.82; N, 11.56; found: C, 69.56; H, 5.89; N, 11.47. HRMS (ESI-TOF) m/z: [**1d** + H]$^+$ calcd for $C_{14}H_{15}N_2O_2$ 243.1128; found 243.1132.

*(E)-1-(3,4-Dimethoxystyryl)isoquinoline (**1e**).* The residue was purified by column chromatography (SiO_2; benzene−ethyl acetate going from 1:0 to 80:20; R_f = 0.80); yellow solid, yield 35% (0.63 mmol, 184 mg), mp 134−137 °C (lit. mp 136−137 °C).[34] ^{1}H NMR (acetone-d_6, 400 MHz) δ: 3.87 (s, 3H, OCH_3), 3.93 (s, 3H, OCH_3), 7.01 (d, 1H, H-5′, J = 8.1 Hz), 7.33 (d, 1H, H-6′, J = 8.5 Hz), 7.53 (br. s, 1H, H-2′), 7.65−7.69 (m, 2H, H-4, H-7), 7.75 (t, 1H, H-6, J = 7.2 Hz), 7.94 (d, 1H, H-5, J = 8.2 Hz), 8.04 (d, 1H, H-b, J_{trans} = 15.4 Hz), 8.15 (d, 1H, H-a, J_{trans} = 15.4 Hz), 8.52 (d, 1H, H-3, J = 5.5 Hz), 8.61 (d, 1H, H-8, J = 8.2 Hz). ^{13}C NMR (acetone-d_6, 101 MHz) δ: 56.2 (*p*-O$\underline{C}H_3$), 56.3 (*m*-O$\underline{C}H_3$), 111.3 (C-2′), 112.8 (C-5′), 120.2 (C-4), 121.4 (C-a), 122.5 (C-6′), 125.6 (C-8), 127.5 (C-8a), 128.1 (C-7), 128.2 (C-5), 130.8 (C-6), 131.1 (C-1′), 136.6 (C-b), 137.8 (C-4a), 143.5 (C-3), 150.8 (C-3′), 151.4 (C-4′), 155.5 (C-1). Anal. calcd for $C_{19}H_{17}NO_2$: C, 78.33; H, 5.88; N, 4.81; found: C, 78.28; H, 5.84; N, 4.75. ESI-MS **1e** in MeCN, m/z: calcd 291.34; found 292.40 [**1e** + H]$^+$.

*(E,E)-2,5-Bis(3,4-dimethoxystyryl)pyrazine (**3a**).* Recrystallized from methanol; orange solid, yield 20% (0.36 mmol, 142 mg), mp 222−224 °C (lit. mp 214 and 229 °C for two polymorphic forms).[35] ^{1}H NMR (DMSO-d_6, 600 MHz) δ: 3.79 (s, 6H, OCH_3), 3.84 (s, 6H, OCH_3), 7.00 (d, 2H, H-5′, J = 8.3 Hz), 7.21 (d, 2H, H-6′, J = 8.5 Hz), 7.31 (d, 2H, H-b, J_{trans} = 16.1 Hz), 7.35 (s, 2H, H-2′), 7.70 (d, 2H, H-a, J_{trans} = 16.0 Hz), 8.68 (s, 2H, H-2, H-5). ^{13}C NMR (DMSO-d_6, 151 MHz) δ: 55.5 (O$\underline{C}H_3$), 109.5 (C-5′), 111.7 (C-2′), 121.3 (C-6′), 122.3 (C-a), 129.1 (C-1′), 133.4 (C-b), 143.1 (C-3), 148.7 (C-3′), 149.0 (C-4′), 149.7 (C-2). Anal. calcd for $C_{24}H_{24}N_2O_4$: C, 71.27; H, 5.98; N, 6.93; found: C, 71.30; H, 6.01; N, 6.98. ESI-MS **3a** in MeCN, m/z: calcd 404.46; found 405.60 [**3a** + H]$^+$.

*(E,E)-4,6-Bis(3,4-dimethoxystyryl)pyrimidine (**3b**).* Purified by column chromatography (SiO_2, benzene−ethyl acetate 10:1, R_f = 0.64) and then recrystallized from methanol; yellow solid, yield 23% (0.41 mmol, 170 mg), mp 128−131 °C. ^{1}H NMR (acetone-d_6, 400 MHz) δ: 3.86 (s, 6H, OCH_3), 3.90 (s, 6H, OCH_3), 7.01 (d, 2H, H-5′, J = 8.3 Hz), 7.12 (d, 2H, H-a, J_{trans} = 15.9 Hz), 7.23 (d, 2H, H-6′, J = 8.2 Hz), 7.36 (s, 2H, H-2′), 7.48 (s, 1H, H-5), 7.92 (d, 2H, H-b, J_{trans} = 16.1 Hz), 8.97 (s, 1H, H-2). ^{13}C NMR (acetone-d_6, 101 MHz) δ: 56.2 (-O$\underline{C}H_3$), 111.0 (C-2′), 112.6 (C-5′), 116.7 (C-5), 122.7 (C-6′), 124.9 (C-a), 129.9 (C-3′), 137.5 (C-b), 150.7 (C-1′), 151.8 (C-4′), 159.4 (C-2), 164.0 (C-4). Anal. calcd for $C_{24}H_{24}N_2O_4$: C, 71.27; H, 5.98; N, 6.93; found: C, 71.15; H, 5.95; N, 6.88. ESI-MS **3b** in MeCN, m/z: calcd 404.46; found 405.50 [**3b** + H]$^+$. HRMS (ESI-TOF) m/z: [**3b** − H]$^+$ calcd for $C_{24}H_{23}N_2O_4$ 403.1652; found 403.1645.

General Procedure for the Synthesis of the Photocyclization Products (2a, 2d, 2e, *E*-4a, and *E*-4b). A solution of the substrate (30.0 mg; **1a**: 0.12 mmol, **1d**: 0.12 mmol, **1e**: 0.10 mmol, **3a**: 0.07 mmol, **3b**: 0.07 mmol) in acetonitrile (1 mM) was irradiated in an immersion well with a Hg photoreactor (125 W), and the reaction was monitored photometrically. When a maximum conversion was reached, the solvent was removed in vacuum, and the residue was washed with hexane and recrystallized from MeOH with addition of $HClO_4$ to give the photocyclization products **2a**, **2d**, **2e**, *E*-**4a**, and *E*-**4b** as perchlorate salts.

*8,9-Dimethoxypyrazino[1,2-a]quinolin-11-ium Perchlorate (**2a**).* Brownish solid, yield 39% (0.05 mmol, 17.0 mg), mp 280−282 °C

DOI: 10.1021/acs.joc.6b01695
J. Org. Chem. 2016, 81, 9075−9085

(dest). ^{1}H NMR (CD_3CN, 600 MHz) δ: 4.11 (s, 3H, 3′-OCH_3), 4.22 (s, 3H, 4′-OCH_3), 7.79 (s, 1H, H-2′), 8.09 (s, 1H, H-5′), 8.34 (d, 1H, H-a, J = 8.7 Hz), 8.83 (d, 1H, H-b, J = 8.7 Hz), 9.00 (d, 1H, H-5,, J = 4.8 Hz), 9.57 (d, 1H, H-6, J = 4.8 Hz), 9.79 (s, 1H, H-3). ^{13}C NMR (CD_3CN, 151 MHz) δ: 57.8 (8-O$\underline{C}H_3$), 58.4 (9-O$\underline{C}H_3$), 99.2 (C-10), 109.7 (C-7), 120.0 (C-5), 123.2 (C-1), 126.9 (C-6a), 130.8 (C-10a), 135.2 (C-4a), 140.3 (C-6), 141.3 (C-2), 154.7 (C-4), 154.8 (C-8), 157.5 (C-9). Anal. calcd for $C_{14}H_{13}ClN_2O_6$: C, 49.35; H, 3.85; N, 8.22; found: C, 49.31; H, 3.95; N, 8.30. HRMS (ESI-TOF) m/z: [**2a**]$^+$ calcd for $C_{14}H_{13}N_2O_2$ 241.0972; found 241.0972.

*8,9-Dimethoxypyridazino[1,6-a]quinolin-11-ium Perchlorate (**2d**).* Brown solid, yield 57% (0.07 mmol, 23.9 mg), mp 183−186 °C (dest). ^{1}H NMR (DMSO-d_6, 600 MHz) δ: 4.08 (s, 3H, 8-OCH_3), 4.15 (s, 3H, 9-OCH_3), 7.96 (s, 1H, H-7), 8.30 (dd, 1H, H-3, J = 8.8 Hz; 4.8 Hz), 8.39 (d, 1H, H-5, J = 8.8 Hz), 8.55 (s, 1H, H-10), 8.95 (d, 1H, H-6, J = 8.8 Hz), 9.05 (d, 1H, H-4, J = 8.8 Hz), 9.62 (d, 1H, H-2, J = 4.4 Hz). ^{13}C NMR (DMSO-d_6, 151 MHz) δ: 56.6 (8-O$\underline{C}H_3$), 56.8 (9-O$\underline{C}H_3$), 98.5 (C-10), 108.0 (C-7), 120.5 (C-5), 124.5 (C-6a), 127.3 (C-3), 133.9 (C-10a), 135.8 (C-4), 138.7 (C-6), 140.5 (C-4a), 150.9 (C-2), 152.3 (C-8), 155.3 (C-9). Anal. calcd for $C_{14}H_{13}ClN_2O_6$: C, 49.35; H, 3.85; N, 8.22; found: C, 49.59; H, 3.91; N, 8.38. HRMS (ESI-TOF) m/z: [**2d**]$^+$ calcd for $C_{14}H_{13}N_2O_2$ 241.0972; found 241.0968.

*2,3-Dimethoxyisoquinolino[2,1-a]quinolinium Perchlorate (**2e**).* Orange solid, yield 50% (0.05 mmol, 19.5 mg), mp 327−329 °C (dest). ^{1}H NMR (CD_3CN, 400 MHz) δ: 4.11 (s, 3H, 3-OCH_3), 4.25 (s, 3H, 2-OCH_3), 7.75 (s, 1H, H-4), 8.08 (s, 1H, H-1), 8.10 (t, 1H, J = 7.7 Hz, H-8), 8.16 (t, 1H, J = 7.0 Hz, H-9), 8.27 (d, 1H, J = 8.2 Hz, H-10), 8.31 (d, 1H, J = 7.7 Hz, H-11), 8.80 (d, 1H, J = 9.2 Hz, H-5), 9.01 (d, 1H, J = 8.2 Hz, H-7), 9.02 (d, 1H, J = 9.2 Hz, H-6), 9.52 (d, 1H, J = 7.7 Hz, H-12). ^{13}C NMR (CD_3CN, 101 MHz) δ: 57.5 (3-O$\underline{C}H_3$), 58.2 (2-O$\underline{C}H_3$), 100.0 (C-1), 109.7 (C-4), 117.2 (C-6), 123.7 (C-11), 124.6 (C-4a), 127.1 (C-7, C-7a), 127.3 (C-12), 129.1 (C-10), 132.3 (C-8), 133.1 (C-10a), 133.3 (C-1a), 135.4 (C-9), 139.8 (C-5), 143.7 (C-6a), 153.0 (C-3), 157.2 (C-2). Anal. calcd for $C_{19}H_{16}ClNO_6$: C, 58.55; H, 4.14; N, 3.59; found: C, 58.48; H, 4.09; N, 3.57. ESI-MS **2e** in MeCN, m/z: calcd 290.34; found 290.10 [**2e**]$^+$. HRMS (ESI-TOF) m/z: [**2e**]$^+$ calcd for $C_{19}H_{16}NO_2$ 290.1176; found 290.1172.

*(E)-2-(3,4-Dimethoxystyryl)-8,9-dimethoxypyrazino[1,2-a]quinolin-11-ium Perchlorate (E-**4a**).* Red solid, yield 25% (0.02 mmol, 10.1 mg), mp 289−292 °C (dest). ^{1}H NMR (CD_3CN, 600 MHz) δ: 3.86 (s, 3H, 4′-OCH_3), 3.90 (s, 3H, 3′-OCH_3), 4.10 (s, 3H, 8-OCH_3), 4.26 (s, 3H, 9-OCH_3), 7.00 (d, 1H, H-5′, J = 8.2 Hz), 7.27 (d, 1H, H-6′, J = 8.2 Hz), 7.29 (s, 1H, H-2′ Hz), 7.48 (d, 1H. H-b, J_{trans} = 15.8 Hz), 7.72 (s, 1H, H-7), 8.02 (d, 1H, H-a, J_{trans} = 15.7 Hz), 8.08 (s, 1H, H-10), 8.26 (d, 1H, H-5, J = 8.8 Hz), 8.65 (d, 1H, H-6, J = 8.7 Hz), 9.38 (s, 1H, H-1), 9.67 (s, 1H, H-4). ^{13}C NMR (CD_3CN, 151 MHz) δ: 56.7 (3′-O$\underline{C}H_3$), 56.8 (4′-O$\underline{C}H_3$), 58.0 (8-O$\underline{C}H_3$), 58.7 (9-O$\underline{C}H_3$), 99.4 (C-10), 110.0 (C-7), 111.2 (C-2′), 113.0 (C-5′), 120.5 (C-1), 120.6 (C-b), 121.1 (C-a), 121.4 (C-5), 123.3 (C-6′), 127.3 (C-6a), 129.8 (C-1′), 130.9 (C-10a) 133.5 (C-4a), 139.0 (C-6), 150.2 (C-2), 150.8 (C-3′), 152.4 (C-4′), 155.0 (C-4), 155.9 (C-8), 157.5 (C-9). Anal. calcd for $C_{24}H_{23}ClN_2O_8$: C, 57.32; H, 4.61; N, 5.57; found: C, 57.38; H, 4.59; N, 5.59. HRMS (ESI-TOF) m/z: [*E*-**4a**]$^+$ calcd for $C_{24}H_{23}N_2O_4$ 403.1652; found 403.1656.

*(E)-2-(3,4-Dimethoxystyryl)-8,9-dimethoxypyrimido[1,6-a]quinolin-11-ium Perchlorate (E-**4b**).* Red solid, yield 51% (0.04 mmol, 18.3 mg), mp 340−345 °C (dest). ^{1}H NMR (DMSO-d_6, 600 MHz) δ: 3.85 (s, 3H, 3′-OCH_3), 3.89 (s, 3H, 4′-OCH_3), 4.03 (s, 3H, 8-OCH_3), 4.17 (s, 3H, 9-OCH_3), 7.09 (d, 1H, H-5′, J = 8.2 Hz), 7.40 (d, 1H, H-6′, J = 8.0 Hz), 7.49 (s, 1H, H-2′), 7.56 (d, 1H. H-a, J_{trans} = 15.5 Hz), 7.88 (s, 1H, H-7), 8.10 (d, 1H, H-5, J = 8.2 Hz), 8.13 (d, 1H, H-b, J_{trans} = 15.5 Hz), 8.34 (s, 1H, H-4), 8.54 (s, 1H, H-10), 8.70 (d, 1H, H-6, J = 8.2 Hz), 10.84 (s, 1H, H-1). ^{13}C NMR (DMSO-d_6, 151 MHz) δ: 55.7 (3′-O$\underline{C}H_3$, 4′-O$\underline{C}H_3$), 56.4 (8-O$\underline{C}H_3$), 57.4 (9-O$\underline{C}H_3$), 99.2 (C-10), 109.4 (C-7), 110.4 (C-2′), 111.8 (C-5′), 115.9 (C-4), 119.6 (C-5), 121.7 (C-a), 122.4 (C-6a), 123.6 (C-6′), 127.9 (C-1′), 129.3 (C-6), 139.9 (C-10a) 141.2 (C-b), 144.4 (C-4a, C-1), 149.2 (C-3′), 151.0 (C-8), 151.4 (C-4′), 154.6 (C-9), 156.3 (C-3). Anal. calcd for $C_{24}H_{23}ClN_2O_8$: C, 57.32; H, 4.61; N, 5.57; found: C, 57.40; H, 4.64; N, 5.60. HRMS (ESI-TOF) m/z: [*E*-**4b**]$^+$ calcd for $C_{24}H_{23}N_2O_4$ 403.1652; found 403.1648.

Photochemical Studies. The solutions of **1a**−**1e** and **3a**, **3b** (c = 20 μM) in acetonitrile or water were irradiated either with filtered light (λ > 295 nm) or with full light of a high-pressure mercury vapor lamp (120 W). Individual lines of the lamp emission spectrum (λ = 365, 405 nm) were isolated with glass filters. All photoreactions were carried out in air-saturated solutions under stirring. The analysis of the reaction progress was performed by absorption spectroscopy.

■ ASSOCIATED CONTENT

Supporting Information

The Supporting Information is available free of charge on the ACS Publications website at DOI: 10.1021/acs.joc.6b01695.

^{1}H and ^{13}C NMR spectra, HRMS data for all new compounds, optical spectroscopy and photochemical studies data (PDF)

■ AUTHOR INFORMATION

Corresponding Author

*E-mail: berdnikova@chemie-bio.uni-siegen.de; daria@ineos.ac.ru.

Notes

The authors declare no competing financial interest.

■ ACKNOWLEDGMENTS

Generous support by the Russian Science Foundation (project 16-13-10226) and the Deutsche Forschungsgemeinschaft (project IH24/13-1) is gratefully acknowledged. T. A. thanks the Deutsche Akademische Austauschdienst (project 57130097). We thank Ms. Jennifer Hermann for technical assistance.

■ REFERENCES

(1) *The Cystic Fibrosis Transmembrane Conductance Regulator*; Kirk, K. L., Dawson, D. C., Eds.; Kluwer Academic/Plenum Publishers: New York, 2003.

(2) Bernier, V.; Lagacé, M.; Bichet, D. G.; Bouvier, M. *Trends Endocrinol. Metab.* **2004**, *15*, 222.

(3) (a) Becq, F.; Mettey, Y.; Gray, M. A.; Galietta, L. J. V.; Dormer, R. L.; Mertenc, M.; Métayé, T.; Chappe, V.; Marivingt-Mounir, C.; Zegarra-Moran, O.; Tarran, R.; Bulteau, L.; Dérand, R.; Pereira, M. M. C.; McPherson, M. A.; Rogier, C.; Joffre, M.; Argent, B. E.; Sarrouilhe, D.; Kammouni, W.; Figarella, C.; Verrier, B.; Gola, M.; Vierfond, J.-M. *J. Biol. Chem.* **1999**, *274*, 27415. (b) Marivingt-Mounir, C.; Norez, C.; Dérand, R.; Bulteau-Pignoux, L.; Nguyen-Huy, D.; Viossat, B.; Morgant, G.; Becq, F.; Vierfond, J.-M.; Mettey, Y. *J. Med. Chem.* **2004**, *47*, 962. (c) Norez, C.; Bilan, F.; Kitzis, A.; Mettey, Y.; Becq, F. *J. Pharmacol. Exp. Ther.* **2008**, *325*, 89.

(4) (a) Vandebrouck, C.; Melin, P.; Norez, C.; Robert, R.; Guibert, C.; Mettey, Y.; Becq, F. *Respir. Res.* **2006**, *7*, 113. (b) Norez, C.; Jayle, C.; Becq, F.; Vandebrouck, C. *Pulm. Pharmacol. Ther.* **2014**, *27*, 38.

(5) Robert, R.; Norez, C.; Becq, F. *J. Physiol.* **2005**, *568*, 483.

(6) Becq, F.; Robert, R.; Pignoux, L.; Rogier, C.; Mettey, Y.; Vierfond, J. M.; Joffre, M.; Marivingt-Mounir, C. Use of benzo[*c*]-quinolizinium derivatives for the treatment of diseases that are linked to smooth muscle cell constriction. U.S. Patent US7897610, 2011.

(7) (a) Ihmels, H.; Faulhaber, K.; Vedaldi, D.; Dall'Acqua, F.; Viola, G. *Photochem. Photobiol.* **2005**, *81*, 1107. (b) Benner, K.; Ihmels, H.; Kölsch, S.; Pithan, P. M. *Org. Biomol. Chem.* **2014**, *12*, 1725.

(8) Mettey, Y.; Vierfond, J.-M.; Baudry, M.; Cochet, C.; Sarrouilhe, D. *Bioorg. Med. Chem. Lett.* **1997**, *7*, 961.

(9) Glover, E. E.; Jones, G. *J. Chem. Soc.* **1958**, 3021.

DOI: 10.1021/acs.joc.6b01695
J. Org. Chem. 2016, 81, 9075−9085

(10) (a) Fozard, A.; Bradsher, C. K. *Chem. Commun.* **1965**, 288. (b) Fozard, A.; Bradsher, C. K. *J. Org. Chem.* **1966**, *31*, 2346. (c) Fozard, A.; Bradsher, C. K. *J. Org. Chem.* **1966**, *31*, 3683.
(11) (a) Arai, S.; Tabuchi, K.; Arai, H.; Yamagishi, H.; Hida, M. *Chem. Lett.* **1991**, *20*, 1355. (b) Arai, S.; Ishikura, M.; Sato, K.; Yamagishi, T. *J. Heterocycl. Chem.* **1995**, *32*, 1081. (c) Arai, S.; Ishikura, M.; Yamagishi, T. *J. Chem. Soc., Perkin Trans. 1* **1998**, *1*, 1561.
(12) Jankowiak, A.; Obijalska, E.; Kaszynski, P.; Pieczonka, A.; Young, V. G., Jr. *Tetrahedron* **2011**, *67*, 3317.
(13) Sinan, M.; Panda, M.; Ghosh, A.; Dhara, K.; Fanwick, P. E.; Chattopadhyay, D. J.; Goswami, S. *J. Am. Chem. Soc.* **2008**, *130*, 5185.
(14) Núñez, A.; Cuadro, A. M.; Alvarez-Builla, J.; Vaquero, J. J. *Org. Lett.* **2007**, *9*, 2977.
(15) Gupta, A. K. *Indian J. Chem.* **2015**, *54B*, 972.
(16) Fedorova, O. A.; Fedorov, Y. V.; Andryukhina, E. N.; Gromov, S. P.; Alfimov, M. V.; Lapouyade, R. *Org. Lett.* **2003**, *5*, 4533.
(17) Fedorova, O. A.; Gulakova, E. N.; Fedorov, Yu. V.; Lobazova, I. E.; Alfimov, M. V.; Jonusauskas, G. *J. Photochem. Photobiol., A* **2008**, *196*, 239.
(18) Berdnikova, D.; Fedorova, O.; Gulakova, E.; Ihmels, H. *Chem. Commun.* **2012**, *48*, 4603.
(19) Gulakova, E. N.; Berdnikova, D. V.; Aliyeu, T. M.; Fedorov, Y. V.; Godovikov, I. A.; Fedorova, O. A. *J. Org. Chem.* **2014**, *79*, 5533.
(20) Fedorov, Y. V.; Tkachenko, S. V.; Chernikova, E.; Yu; Godovikov, I. A.; Fedorova, O. A.; Isaacs, L. *Chem. Commun.* **2015**, *51*, 1349.
(21) Berdnikova, D. V.; Aliyeu, T. M.; Paululat, T.; Fedorov, Y. V.; Fedorova, O. A.; Ihmels, H. *Chem. Commun.* **2015**, *51*, 4906.
(22) Budyka, M. F.; Li, V. M.; Gavrishova, T. N.; Potashova, N. I. *High Energy Chem.* **2015**, *49*, 158.
(23) Granzhan, A.; Ihmels, H. *Synlett* **2016**, *27*, 1775.
(24) (a) Horspool, W.; Lenci, F. *CRC Handbook of Organic Photochemistry and Photobiology*; 2nd ed.; CRC Press: Boca Raton, FL, 2004. (b) Shugar, D.; Fox, J. J. *Biochim. Biophys. Acta* **1952**, *9*, 199.
(25) (a) Huang, Y.; Cheng, T.; Li, F.; Luo, C.; Huang, C.-H.; Cai, Z.; Zeng, X.; Zhou, J. *J. Phys. Chem. B* **2002**, *106*, 10031. (b) Strehmel, B.; Seifert, H.; Rettig, W. *J. Phys. Chem. B* **1997**, *101*, 2232. (c) Ephardt, H.; Fromherz, P. *J. Phys. Chem.* **1989**, *93*, 7717. (d) Rettig, W. *Angew. Chem., Int. Ed. Engl.* **1986**, *25*, 971.
(26) (a) Rescifina, A.; Zagni, C.; Varrica, M. G.; Pistara, V.; Corsaro, A. *Eur. J. Med. Chem.* **2014**, *74*, 95. (b) Banerjee, S.; Veale, E. B.; Phelan, C. M.; Murphy, S. A.; Tocci, G. M.; Gillespie, L. J.; Frimannsson, D. O.; Kelly, J. M.; Gunnlaugsson, T. *Chem. Soc. Rev.* **2013**, *42*, 1601. (c) Mukherjee, A.; Sasikala, W. D. *Adv. Protein Chem. Struct. Biol.* **2013**, *92*, 1. (d) Wang, X.; Guo, Z. *Chem. Soc. Rev.* **2013**, *42*, 202. (e) Xie, Y.; Tam, V. K.; Tor, Y. In *The chemical biology of nucleic acids*; Mayer, G., Ed.; John Wiley & Sons: Chichester, 2010. (f) Haq, I. In *Nucleic acids in chemistry and biology*; Blackburn, G. M., Gait, M. J., Loakes, D., Williams, D. M., Eds.; Royal Society of Chemistry: Cambridge, 2006. (g) Ihmels, H.; Otto, D. *Top Curr. Chem.* **2005**, *258*, 161.
(27) (a) McGhee, J. D.; von Hippel, P. H. *J. Mol. Biol.* **1974**, *86*, 469. (b) Stootman, F. H.; Fisher, D. M.; Rodger, A.; Aldrich-Wright, J. R. *Analyst* **2006**, *131*, 1145.
(28) Ihmels, H.; Otto, D.; Dall'Acqua, F.; Faccio, A.; Moro, S.; Viola, G. *J. Org. Chem.* **2006**, *71*, 8401.
(29) (a) Fukui, K.; Tanaka, K.; Fujitsuka, M.; Watanabe, A.; Ito, O. *J. Photochem. Photobiol., B* **1999**, *50*, 18. (b) Murphy, C. J.; Arkin, M. R.; Ghatlia, N. D.; Bossmann, S.; Turro, N. J.; Barton, J. K. *Proc. Natl. Acad. Sci. U. S. A.* **1994**, *91*, 5315.
(30) Norden, B.; Rodger, A.; Dafforn, T. *Linear Dichroism and Circular Dichroism*; RSC Publishing: Cambridge, 2010.
(31) Hannah, K. C.; Armitage, B. A. *Acc. Chem. Res.* **2004**, *37*, 845.
(32) (a) Kumar, C. V.; Turner, R. S.; Asuncion, E. H. *J. Photochem. Photobiol., A* **1993**, *74*, 231. (b) Sahoo, D.; Bhattacharya, P.; Chakravorti, S. *J. Phys. Chem. B* **2010**, *114*, 2044.
(33) Hong, Y.; Lam, J. W. Y.; Tang, B. Z. *Chem. Soc. Rev.* **2011**, *40*, 5361.
(34) Bahner, C. T.; Rives, L. M.; McGaha, S. W.; Rutledge, D.; Ford, D.; Gooch, E.; Westberry, D.; Ziegler, D.; Ziegler, R. *Arzneimittelforschung* **1981**, *31*, 404.
(35) Collas, A.; Bagrowska, I.; Aleksandrzak, K.; Zeller, M.; Blockhuys, F. *Cryst. Growth Des.* **2011**, *11*, 1299.

DOI: 10.1021/acs.joc.6b01695
J. Org. Chem. 2016, 81, 9075−9085